UNDERSTANDING OPERATING PRINCIPLES AND PROCESSIVITY OF MOLECULAR MOTORS*

Bartosz Lisowski, Michał Świątek, Michał Żabicki
Ewa Gudowska-Nowak

The Marian Smoluchowski Institute of Physics
and
The Mark Kac Complex Systems Research Center
Jagiellonian University, Reymonta 4, 30-059 Kraków, Poland

(Received April 23, 2012)

Motor proteins, sometimes referred to as *mechanoenzymes*, are a group of proteins that maintain a large part of intracellular motion. Being *enzymes*, they undergo chemical reactions leading to energy conversion and changes of their conformation. Being *mechanodevices*, they use the chemical energy to perform mechanical work, leading to the phenomena of motion. Over the past 20 years a series of novel experiments (*e.g.* single molecule observations) has been performed to gain the deeper knowledge about chemical states of molecular motors as well as their dynamics in the presence or absence of an external force. At the same time, many theoretical models have been proposed, offering various insights into the nano-world dynamics. They can be divided into three main categories: mechanochemical models, ratchet models and molecular dynamics simulations. We demonstrate that by combining those complementary approaches a deeper understanding of the dynamics and chemistry of the motor proteins can be achieved. As a working example, we choose kinesin — a motor protein responsible for directed transport of organelles and vesicles along microtubule tracts.

DOI:10.5506/APhysPolB.43.1073
PACS numbers: 87.10.–e, 87.18.–h

1. Introduction

Problem of transport is fundamental for understanding efficient functioning of complex systems. Regardless of whether one studies social interactions among ants, networks of municipal delivery of goods, coupled systems of electrical conductors or "machinery" of living cells, a comprehensive insight into their structure and operation properties can be gained only by unraveling the dynamical features of a system under consideration.

* Presented at the XXIV Marian Smoluchowski Symposium on Statistical Physics, "Insights into Stochastic Nonequilibrium", Zakopane, Poland, September 17–22, 2011.

For modern cell biology and biotechnology, understanding how cells maintain and control their inner environment is one of the most fundamental goals. For physicists, chemists and nano-engineers studying the most optimal and evolution-optimized bio-machines creates an unique way for conceptual advancement of design, fabrication and manipulation of synthetic nano-devices, such as *lab on a chip* or dedicated nano-robots [1, 2].

Chemical models of molecular motors focus on the Markov chain, kinetic description of the reaction cycles responsible for the mechanical transitions. So-called ratchet models are mostly based on sets of Langevin equations and treat the kinesin dimer as two linked Brownian particles moving in a periodic potential. Molecular dynamics (MD) models approach the problem from the low level dynamics of single or grouped molecules, based on information obtained from crystallographical data.

In this work, we briefly review results of our studies aimed to understand processivity of a molecular motor by combining results of simulations of a statistical mechanochemical device with a ratchet model and molecular dynamics investigations of an elastic motor structure.

1.1. Molecular motors

Molecular motors are a class of highly specialized molecules, present in both prokaryotic and eukaryotic cells. Their role is to convert energy into mechanical work. It is this unique feature that makes them invaluable for essential biological processes such as coordinated intracellular transport, muscle contraction, transcription, mitosis and ATP[1] synthesis, to name only few. The source of energy they use, as well as their function, differ between distinct classes of motors. Here, we focus on an eukaryotic cytoskeletal motor protein, kinesin-1 (so-called conventional kinesin).

Kinesins take care of internal transport needs of a cell: they carry liposomes containing various substances (*e.g.* neurotransmitters) and also organelles (*e.g.* mitochondria). They do so by literally walking on the biopolymer microtubule, an important part of the cytoskeleton, forming a molecular tract. Microtubule is a polymeric tube, consisting of alternately arranged α- and β-tubulin dimers [3]. The whole structure is polarized: the so-called *minus* end of the tube, associated with the structure called microtubule-organizing center (MTOC) and localized most often near the nucleus, is stable while the second, called *plus* end is labile and may be assembled or disassembled, depending on the cell's needs. This variability of the *plus* end is called dynamic instability [4]. Single kinesin-1 molecule (see Fig. 1) consists of two **motor domains** (*heads*), binding to the microtubule, a **stalk**

[1] Adenosine-5'-triphosphate.

responsible for attaching the cargo and elastic **neck linkers**, connecting the heads with the stalk. Heads are those parts of the protein, where the production of the source of energy to the motor (catalyzed ATP hydrolysis) takes place.

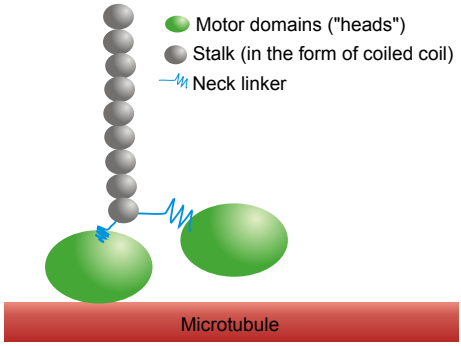

Fig. 1. Schematic representation of a kinesin-1 motor protein. It consists of two **motor domains** (*heads*), binding to the microtubule; a **stalk** responsible for attaching a cargo and **neck linkers** — polypeptides containing over a dozen of amino acids each, connecting both heads with the stalk.

Accordingly, molecular motors are powered by the chemical energy, stored in the form of phosphate bonds in ATP molecules. Hydrolyzing those bonds triggers the changes of their conformation and allows them to perform mechanical work. In the case of kinesin-1, each successfully hydrolyzed ATP molecule allows to perform one step towards the *plus* end of the microtubule or, extremely rarely, towards its *minus* end. This broken symmetry between the frequency of forward and backward steps is an effect of kinesin's **directionality**. For many mechanoenzymes, observed over the long time scale, the number of steps taken in one direction is greater than the number of steps taken in the other one. Directionality is a consequence of a structure of both, motor and its track, and can be also observed in coordinated actions of many collaborating groups of motors. One of the best examples is the bidirectional axonal transport, where plus-end oriented kinesins and minus-end oriented dyneins move their cargos from cell body (*perikaryon*) to axon back and forth.

The regular structure of microtubule affects the dynamics of kinesin in yet another way: because the head may dock itself to the microtubule only in a specific manner (most of the head attaches to β-tubulin monomers), each step is of the same size, *i.e.* about 8 nm for the movement of the center-of-mass, which corresponds to microtubule's periodicity.

2. Molecular dynamics

The behavior of a protein amino acid chain is roughly similar to that of a biopolymer. As such, it comes as no surprise that a specific fragment of a kinesin chain is responsible for spring-like relative movement of kinesin heads. Such a fragment, present in each kinesin head, is known as a **neck linker**. One typical kinesin molecule consists of two identical amino acid chains[2]. N-terminus of each chain is the core of each kinesin head that forms around a single Mg^{2+} ion. More than 300 residues belongs to a kinesin head. Towards the C-terminus, the amino acid chain takes upon a shape of a helix. The helixes of two different chains intertwine, forming a stalk (*cf.* Fig. 1). The neck linker is a part of the amino acid chain situated between a head and a stalk. Only when it forms the outer edge of the kinesin head central β-sheet, does it develop a rigid conformation. Otherwise, a neck linker attached to the free kinesin head remains unstructured. In a typical kinesin structure, neck linker spans from 338th to 354th residue [5] and has a mass of about 2 kDa[3]. In most biomechanical models, those two linkers are treated as harmonic springs. Nevertheless, since the amino acid sequence is often significantly varied, it is unclear if such an approach is correctly justified. Our aim was, therefore, to determine whether and to what extend, the structure of the linker can be approximated by the elasticity of the worm-like-chain (WLC) model [6].

The elasticity of unstructured biopolymers is frequently described by the WLC model which has been claimed to predict correctly the force extension properties of polypeptide chains (see discussion in [7]). Within this approach, the force required to extend a polymer with a given contour length L_c[4] and persistence length L_p to a given end-to-end distance x can be approximated by the formula

$$f = \frac{k_B T}{L_p}\left[\frac{1}{4}\left(1-\frac{x}{L_c}\right)^{-2} + \frac{x}{L_c} - \frac{1}{4}\right], \tag{1}$$

where $k_B T$ is energy measured in Boltzmann units of temperature. In order to perform a suitable test, we have studied **elasticity** of the linker by performing MD simulations (`GROMACS 4.5.4` [8]) on a structure of an

[2] Amino acids owe their name to the presence of two characteristic groups: an amine group ($-NH_2$) and a carboxyl group (–COOH). When forming a peptide, a peptide bond is created by joining the amine group of one amino acid to the carboxyl group of the subsequent one. A final product of this condensation reaction is a chain that has a free amine group on one end and a free carboxyl group on the other. Those ends are called N-terminus and C-terminus, respectively.

[3] An atomic mass unit of 1 dalton (Da) corresponds to 1.661×10^{-27} kg.

[4] The contour length of a polypeptide is equal to the number of amino acids times distance along the chain per amino acid [6].

idealized polymer (a model alanine structure) and on a sequence of a neck linker domain obtained from the Protein Data Bank (PDB). Starting coordinates for a linker structure have been obtained from the sequence of a kinesin-like protein KIF3B, downloaded from the existent PDB database (`ID: 3B6U`). Both structures (alanine and the 3B6U linker) have been further used to determine an effective mechanic potential function V of a system containing N atoms, described as

$$\begin{aligned} V \;=\; & \sum_{\text{bonds}} \frac{k_i}{2}\left(x_i - x_{i,0}\right)^2 + \sum_{\text{angles}} \frac{k_i}{2}\left(\theta_i - \theta_{i,0}\right)^2 \\ & + \sum_{\text{torsions}} \frac{V_n}{2}\left[1 + \cos\left(n\omega - \gamma\right)\right] \\ & + \sum_{i}^{N} \sum_{j=i+1}^{N} \left(4\epsilon_{ij} \left[\left(\frac{\sigma_{ij}}{r_{ij}}\right)^{12} - \left(\frac{\sigma_{ij}}{r_{ij}}\right)^{6} \right] + \frac{q_i q_j}{4\pi\epsilon_0 r_{ij}} \right) . \end{aligned} \tag{2}$$

Here, x_i is a symbol of an ith bond length, θ_i is a symbol of an ith angle value while $x_{i,0}$ and $\theta_{i,0}$ are their respective reference values. V_n is a parameter that gives information about rotation barriers of torsion angle ω, while k_i refers to a ith force constant. ϵ_{ij} is a minimal value of the Van der Waals potential between atoms i and j, r_{ij} represents a distance between these centers and σ_{ij} is a distance between them when Van der Waals potential value is 0. Symbols q_i and q_j refer to charges of ith and jth atoms and ϵ_0 stands for a dielectric constant. Since bond lengths, bond- and dihedral angles can be rephrased in terms of position vectors $\vec{\boldsymbol{r}}$, changes in the position of atoms are evaluated by solving Newton equation of motion with forces $\vec{\boldsymbol{F}}_i = -\frac{\partial V}{\partial \vec{\boldsymbol{r}}_i}$.

For the purpose of modeling, in course of simulations, both linker and alanine sequences have been put into boxes filled (uniformly) with water and subject to periodic boundary conditions. Equilibrium runs of 50 ps have been carried out for each sequence. A single simulation step has covered 2×10^{-3} ps and each simulation has been running for 100 ps. The simulations have been performed at constant pressure of 100 kPa and at temperature of 300 K. The methods used to control temperature (separately, for solvent and solute) and pressure of the system have been adjusted to the Berendsen and Parinello–Rahman procedures [8], respectively. Results shown in Fig. 2 have been averaged over 6 simulations for each molecule.

Only that part of the KIF3B structure which contained a sequence identified as a neck linker [5] has been simulated. Additionally, constant force f ($f = 216$ pN) has been applied, pointing from the neck linker central residue's center-of-mass towards either one of the ends. Similar procedure has been used for a simulation of a comparative sequence consisting of alanine residues. The results of those simulations are depicted in Fig. 2.

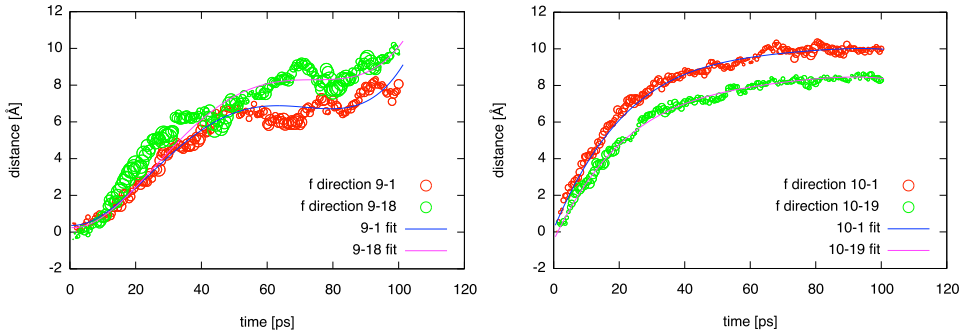

Fig. 2. Distance changes of alanine (left plot) and neck linker (right plot) chains. Our aim was to study elasticity of the linker by performing MD simulations of a protein head's fragment obtained from KIF3B structure stored in PDB database (`ID: 3B6U`). The (constant) external forces applied are set to 216 pN. Simulation steps are 2×10^{-3} ps and length of each simulation is 100 ps. Results shown in the graph are averaged over 6 simulations for each molecule. The radius of a circle around each point corresponds to the standard deviation from the mean.

Left plot of Fig. 2 displays distance changes for alanine consisting of 19 amino acid residues. Here, "f direction 10–1" denotes the force applied to 1st residue, pushing towards that position from the 1th residue while force "f direction 10–19" denotes action of the force applied to 19th residue pushing from the same center (position of the 10th residue). Analogously, right plot illustrates distance changes for a sequence consisting of 18 amino acids of the **neck linker**. Label "f direction 9–1" denotes the force applied to 1st residue from the 9th residue while "f direction 9–18" denotes the force of the same intensity applied to 18th residue and pushing from the 9th one. The radius of a circle around each point corresponds to the standard deviation. Distance changes are calculated for distances between C_α atoms of residues being pushed away and atoms C_α of those residues that are a reference for applied forces (9th and 10th residues for alanine and neck linker sequences, respectively).

If the contour length L_c is made of n units of an approximately same length l, then by the Kuhn's formula $l = 2L_\mathrm{p}$, so that in the linear regime of the extension, one can approximate Eq. (1) with the Hook force,

$$f \approx \frac{3k_\mathrm{B}T}{lL_\mathrm{c}}x\,. \tag{3}$$

The motion of the linker center-of-mass can be then written as

$$M\frac{dv}{dt} = \frac{3k_\mathrm{B}T}{lL_\mathrm{c}}(x_0 - x) - \gamma_\mathrm{L}v + \xi(t)\,, \tag{4}$$

with M standing for the mass of the extended polymer/linker, ξ being the Brownian white noise mimicking thermal fluctuations, $x_0 - x$ denoting a relative position and γ_{L} describing the drag coefficient. With the extension satisfying $dx/dt = v$, and by assuming the overdamped motion in the center of linker's mass, this equation predicts a linear $x(t)$ dependence. As visualized in Fig. 2, stretching applied to the alanine sequence results, in both its parts, in a semi-linear response typical for a harmonic spring curve, but only up to a certain point in time (about 50 ps), after which a leveling-off is observed. In contrast, for times up to about 30 ps, stretching of each half of the neck linker structure results in extensions very well following expectations derived from a harmonic spring model. Still, both linker halves do not behave identically and their elasticity coefficients are systematically different. One of the halves is able to stretch to a longer distance than the other, even though they consist of the same number of residues.

Altogether, these results show that our method can detect spring-like behavior of a neck linker and that such behavior is not an universal feature in amino acid chains. Furthermore, they suggest that distance changes between kinesin heads in models describing kinesin movement should be represented in more complex way than stretching of a single spring.

3. Chemical models

Conformational changes within the kinesin's structure influence chemical kinetics of reaction cycles, catalyzed by the motor. For this reason, one of the approaches towards motor proteins modeling is a chemomechanical one. It is based on the results of experiments, in which the enzymes' working cycles can be determined. Knowing all the reactions that may occur on the active sites of kinesin's motor domains, it is possible to estimate the rate of the sequence of transitions. One can then quantitatively describe the chemomechanical coupling, that is a connection between energy providing chemical reactions and conformational changes they trigger, leading to directed stepping along microtubule.

Fig. 3 shows a schematic representation of an exemplary kinesin's chemomechanical cycle. Ovals represent two kinesin's heads, left — the rear one, right — the leading one. Such representation is consistent with the hand-over-hand walking model [9], where heads interchange their positions sequentially. Each of the heads may be found in four chemical states:

- **E**, when the motor domain is empty,
- **D**, when the motor domain is occupied by ADP[5],

[5] ADP — adenosine diphosphate.

- **T**, when the motor domain is occupied by ATP, and
- **P**, when the motor domain is occupied by an ADP–P complex[6].

State **P** may be neglected, since its lifetime is very short (that is, inorganic phosphate is released rapidly after the ATP decay) [3]. Transitions among states are related to binding and unbinding the ATP, ADP and P molecules. For example, transition $1 \rightarrow 2$ from Fig. 3 may be deciphered as the binding of one ATP molecule to the leading head of kinesin-1, and the reverse transition $2 \rightarrow 1$ is a release of one ATP molecule from the leading head.

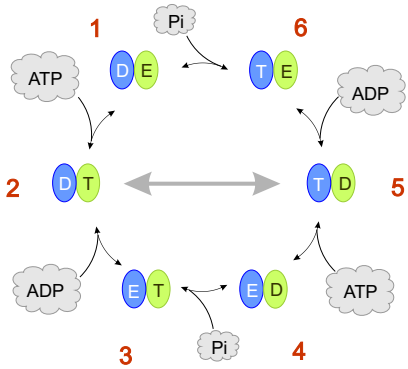

Fig. 3. Kinesin's working cycle, from [10], changed. Thin arrows represent chemical reaction, thicker one — a mechanical step. Ovals stand for kinesin's heads at chemical states E (empty head), D (head with attached adenosine diphosphate ADP) and T (head with adenosine triphosphate ATP), respectively. Clouds represent chemical substrates — ADP, ATP and P (inorganic phosphate). During transition $2 \leftrightarrow 5$ kinesin takes one mechanical step: a forward step, towards the plus end of the microtubule, when $(2 \rightarrow 5)$ or a backstep $(5 \rightarrow 2)$.

It is known that in states **T** and **E** the head is tightly bound to the microtubule, while in state **D** the binding is weak and may be easily broken. This and the results of studies on how the concentration of ATP and ADP impacts on motor's dynamical properties led to conclusion that the mechanical transition (a step) is possible only from **DT** to **TD** states and in reverse. Another important factors that have to be taken into account when constructing schemes of the kinesin working cycle, are the mechanical constraints. It has been shown that the access to motor domain's active place is controlled by the strain of the whole molecule, conditioned by the strain of neck linker [11]. For each chemical state the neck linker's stiffness must be determined and taken into account. It is why the studies similar to those presented in Sec. 2 are so important.

[6] P — inorganic phosphate.

Motor proteins are subjected to many forces of distinct origin, that affect their behavior. In general, for our purpose we may divide them, after Howard [3], into **chemical forces**, resulting from the formation of chemical bonds, and **external mechanical forces**, as the load force exerted on motor-cargo system in optical tweezer experiments. While the first ones may drive kinesin to move in one direction, the latter may favor the opposite direction. A net result of competing forces depends on which force has *greater* effect on the protein's chemomechanical cycle.

Chemical forces reflect the probability of each reaction and their effects, leading to conformational changes and performing mechanical work. As for mechanical forces, the standard way of reflecting their impact on reaction rates originates from the Arrhenius rate theory. In the case of walking kinesin which covers in each mechanical step a distance of $d \approx 8$ nm, the external force F modifies the reaction rate k by a force-dependent transition, so that $k \propto k_0 \exp[\frac{Fd}{k_B T}]$.

While constructing chemomechanical models, one has to include all available biologically relevant data. It sets the background and defines the constraints for the model. Below, we will briefly comment on some ambiguities often found when comparing different chemomechanical models.

After hydrolyzing one ATP molecule and detaching from microtubule, the rear head is subjected to random Brownian motion, that moves it back and forth around the still attached second head[7]. When the head finds itself near the microtubule's next binding site, new bounds may form and dock the head, finishing the forward step. Occasionally it may happen that, after hydrolyzing one ATP molecule, the leading head will detach. The probability that it will move back and dock to the rear free binding place is much smaller than that of rebinding to the same place. However, it is non-zero and such backsteps can occur. What is important, both forward and backward steps (and unbinding–rebinding events, ending with futile hydrolysis and no step, as well) require hydrolysis, or at least attachment of one ATP molecule [12].

Since there are some convincing suggestions that backstepping may play an important role in maximizing motor's speed by increasing its entropy [13], and considering that the stepping ratio, $\frac{n_f}{n_b}$, is experimentally achievable, our goal was to investigate three different theoretical models, used frequently to describe kinesin's behavior: 2-state and 4-state models from [14] and 6-state model from [10] (see Fig. 3).

As can be seen in Fig. 4, the results differ significantly.

[7] It seems likely that the conformation change, which accompanies the detachment of the rear head, can also move this head in a directed manner at a small distance, decreasing the distance it has to cover due to thermal motion and increasing the probability of successful binding in front of the second head. This mechanism is called *a power stroke*.

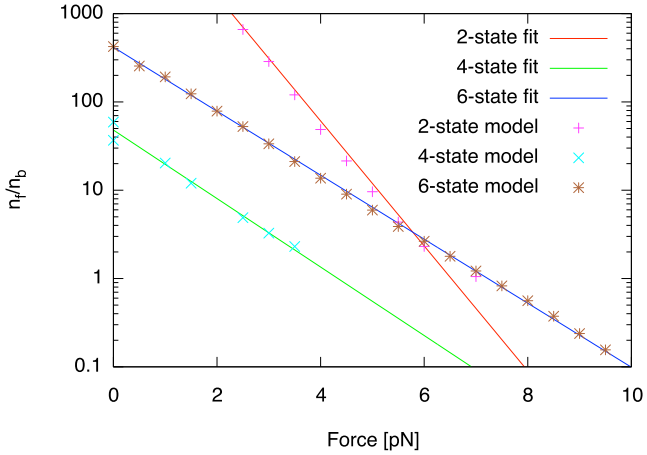

Fig. 4. Step ratio as a function of load force for three (2-state, 4-state and 6-state) models. Parameters of the 2-state and 4-state models are the same as in [14], and those of the 6 state models are from [10] with [ADP] = [P] = 10 μM, [ATP] = 1 mM. n_{f} denotes the number of forward steps, n_{b} — number of backward steps. Each point symbolizes the step ratio obtained after 10^5transitions in the chemomechanical cycle for different values of the force (from 0 to 10 pN, increasing by 0.5 pN for subsequent cycle's series).

In the case of the 2- and 4-state models from [14], the backstepping issue has not been discussed. For the 6-state model [10] the step ratio q has been introduced and defined as $q = \frac{P_2\omega_{25}}{P_5\omega_{52}}$, where P_i is the probability of being in state i of the chemomechanical cycle (see Fig. 3) and ω_{ij} is the rate of a transition from state i to j. When calculating motor's velocity, authors of [10] have also used the parameters connected with the transition from state 2 to state 5 of the proposed chemomechanical cycle, *cf.* Fig. 3. However, this treatment seems rather ambiguous, since the experimental data suggest, that after advancing the rear head in front of the leading one (transition $2 \rightarrow 5$ in Fig. 3), ADP has to be released (transition $5 \rightarrow 6$), allowing the now-leading head to attach firmly to the microtubule. Otherwise, before releasing ADP, a weakly bounded head may easily detach with no additional ATP molecule being hydrolyzed and the head will continue its diffusive search of a free binding site. Such an event should not, in our opinion, be counted as one step. Similar concerns can be brought up with regard to the backsteps (transitions $5 \rightarrow 2$ in Fig. 3).

To check how the definition of a single step, both forward and backward, affects the predictions of the model, we have compared the results of simulations of the chemomechanical cycle of the 6-state model from [10] (see Fig. 3) for three different cases, differing only in the definition of what should be counted for "one step".

Accordingly, in **model 1** all the transitions $2 \rightarrow 5$ were identified as one forward step, while the transitions $5 \rightarrow 2$ as one backward step. In **model 2** we have counted one forward step for the sequence of transitions being $2 \rightarrow 5 \rightarrow 6$ or $2 \rightarrow 5 \rightarrow 4$ (that is, the kinesin's head has been assumed docked after interchanging position with the other head and after another chemical, but not mechanical, transition from state 5 has taken place). Furthermore, one backward step has been identified with the transition sequences $5 \rightarrow 2 \rightarrow 1$ or $5 \rightarrow 2 \rightarrow 3$. In **model 3**, the most rigorous one, a forward step has been counted after each $2 \rightarrow 5 \rightarrow 6$ sequence, while the backward one, after the $5 \rightarrow 2 \rightarrow 1$ sequence has been concluded. This has been in line with the analysis of experimental data described recently by Block's group in [15].

Illustration of our results is displayed in Fig. 5. Number of forward and backward steps performed by the motor influenced by different loads, while simulating models 1, 2 and 3, is shown in Fig. 6.

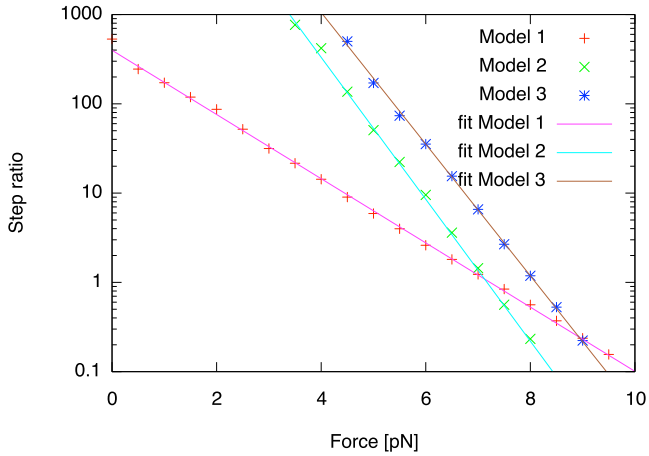

Fig. 5. Step ratio as a function of load force for three models: Model 1, Model 2 and Model 3 (see the text). Parameters of all the models are the same, all as in [10] with [ADP] = [P] = 10 μM, [ATP] = 1 mM. Step ratio is $\frac{n_\mathrm{f}}{n_\mathrm{b}}$, where n_f denotes the number of forward steps, n_b — number of backward steps. Each point symbolizes the step ratio obtained after 10^5 transitions in the chemomechanical cycle for different values of the force (from 0 to 10 pN, increasing by 0.5 pN for subsequent cycle's series).

All simulations were based on the Gillespie algorithm for chemical state transitions [16, 17]. We have treated kinesin's stepping as a Markov chain in which the probability $P_i(t)$ that the motor occupies state i at time t is evolving according to the Master equation

$$\dot{P}_i = -\sum_j P_i \omega_{ij} - P_j \omega_{ji} \,. \tag{5}$$

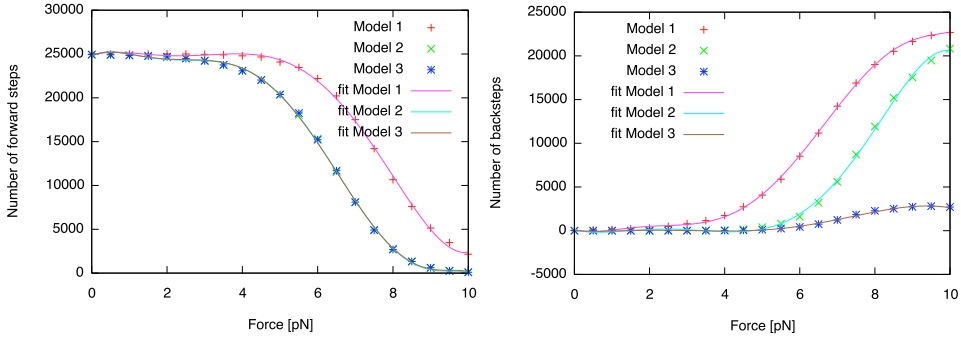

Fig. 6. Number of forward steps (left plot) and backward steps (right plot) as a function of load force for three models: Model 1, Model 2 and Model 3 (see the text). Parameters of all the models are the same, all as in [10] with [ADP] = [P] = 10 μM, [ATP] = 1 mM. Each point was obtained after 10^5 transitions in the chemomechanical cycle for different values of the force (from 0 to 10 pN, increasing by 0.5 pN for subsequent cycle's series).

Rate of a transition from state i to j, ω_{ij}, as well as other parameters were taken from [14] (for the 2-state and 4-state model) and [10] (for the 6-state model and for models 1, 2 and 3), unless the text states differently

$$\omega_{ij} = \kappa_{ij} I_{ij}([X]) \phi_{ij}(F_0)\,. \tag{6}$$

Here, κ_{ij} is rate constant of the transition from i to j, $I_{ij}([X]) = [X]$ and X = ATP, ADP or P and $I_{ij}([X]) = 1$ for the transitions without chemical reactions. $\phi_{ij}(F_0)$ describes the effect of load force F_0 which assumes the following form [10]: $\phi_{25}(F_0) = \exp\left(-\theta \frac{F_0 d}{k_\mathrm{B} T}\right)$ and $\phi_{52}(F_0) = \exp\left[(1-\theta)\frac{F_0 d}{k_\mathrm{B} T}\right]$ for the mechanical transitions and $\phi_{ij}(F_0) = 2\left(1 + \exp\left[\chi_{ij}\frac{F_0 d}{k_\mathrm{B} T}\right]\right)^{-1}$ and $\chi_{ij} = \chi_{ji}$ for the chemical transitions.

Results show that the stepping ratios' ($\frac{n_\mathrm{f}}{n_\mathrm{b}}$) comparison made for different kinesin models may be used as a method of their evaluation and validation of parameters (*e.g.* rate constants) that cannot be obtained experimentally. Moreover, they reveal the importance of defining the critical elements of chemomechanical cycles, especially the sequence of transitions involved in a definition of a forward and backward steps. As justified above, moving the rear head in front of the leading one is not enough to count this action as one forward step. For this, subsequent docking of the head to the microtubule and following chemical transitions are required. One way of solving the ambiguity of the definition of step is to identify it with an irreversible transition as in [15]. However, such an approach depreciates effects connected with molecular crowding, where Brownian movement of undocked

head may be of greater importance than in buffer solutions used for *in vitro* experiments. For example, it is a common knowledge that in overcrowded environment of cell's interior, reaction rates differ significantly from those measured *in vitro* [18].

As presented in Fig. 6, the number as well as the definition of backsteps, significantly affect the value of the stepping ratio and, as a consequence, the estimated motor's velocity. This tendency is observed even for values of load smaller than the stall force[8] $F_S \sim 7$ pN. It is an argument for the theories similar to the one presented by Bier and Cao in [13].

4. Ratchet models

A mechanic motor is a machine that converts some kind of energy into useful mechanical work, and as such it is what we call an engine. Key features of an engine are:

(a) fuel — the kind of energy that is used to perform work;

(b) power — which gives information what kind of work can by done by an engine in a given period of time;

(c) efficiency — the measure of how effectively the provided energy is converted into mechanical work.

For an average macro-motor like a car, an engine is a gas-driven, 120 kW strong device of an efficiency of about 20%. In this work, we discuss efficiencies of much smaller motors operating in a nano-scale of the living cells. The size of molecular motors and their overcrowded environments have a crucial impact on the key features of their dynamics. Kinesin, dynein and other motor proteins work in a dense cell environment, named sometimes "Brownian domain" after work by Magnasco [19]. That statement has been the foundation of using Smoluchowski's idea (a fluctuation-driven ratchet) as an explanatory model for molecular motors [3, 6, 20, 21, 22]. Obviously, in biological realms it is hard to achieve thermal gradients large enough to drive directed motion [20]. There are, however, other ways of providing energy that can result in net movement of a particle. We briefly review them in the forthcoming sections.

4.1. Fluctuation driven ratchets

The first kind of models are based on the external fluctuations of the ratchet-shaped potentials [21]. Those include cyclically turning on/off potentials ("flashing ratchets") or rocking (tilting) potentials mitigated by fluctuating forces (so-called "rocking" or "tilting" ratchets) [23]. This group of

[8] Stall force, F_S, is such a load force, under which the motor cannot operate and stops.

models can be jointly described by a Langevin equation in the form

$$m\ddot{x} + \gamma\dot{x} + \frac{dV(x,t)}{dx} = \xi(t) \ , \tag{7}$$

where $V(x,t)$ is a periodic, asymmetric potential that changes in time and $\xi(t)$ stands for the random Gaussian forcing. In general, for the group of particles with external energy uptake and storage in the form of a depot, the active Brownian motion (ABM) can be modeled by a varying friction coefficient [24,25,26,27,28]. In this class of models friction may become negative at low body's velocity. Langevin equation under those circumstances reads

$$m\ddot{x} + \gamma(\dot{x})\dot{x} = \xi(t) \ , \tag{8}$$

Depending on an approach two different, nonlinear velocity-dependent friction functions are usually postulated. The first one proposed by Schweitzer *et al.* [24] reads

$$\gamma(\dot{x})_{\mathrm{SET}} = \gamma_0 \left(1 - \frac{\beta}{1+\dot{x}^2}\right) \tag{9}$$

with β being a control bifurcation parameter. The model implies negative friction for low velocities within the range $|\dot{x}| < \sqrt{\beta - 1}$ and a "standard" positive value outside this region. The active motion corresponds to the regime $\beta > 1$. Somewhat simpler version of the model is offered by the Rayleigh–Helmholtz friction function [24]

$$\gamma(\dot{x})_{\mathrm{RH}} = \gamma_0 \left(\dot{x}^2 - \alpha\right) \ . \tag{10}$$

Here, friction is negative within the region of $|\dot{x}| < \sqrt{\alpha}$ and becomes zero for $\alpha = \dot{x}^2$. Accordingly, the friction force attains negative values at small speed (it is pumping energy into the system) while at large velocities a cubic term $\dot{x}^3$ dominates. Both models of frictional forces have been used to describe systems with an energy depot [24], which acquires energy from the environment with a rate $q(r)$, stores it as an internal energy $e(t)$ and then provides it for conversion into kinetic energy with a rate $d(v)$

$$\frac{d}{dt}e(t) = q(x) - ce(t) - d(\dot{x})e(t) \, . \tag{11}$$

After taking into account mechanical energy balance, Langevin equation for the depot-based active Brownian particle reads

$$m\ddot{x} + \gamma\dot{x} + \nabla V(x) = d_2 e(t)\dot{x} + \xi(t) \ , \tag{12}$$

where $d_2 = v^2/d(\dot{x})$. Comparing to Eq. (7), the most evident difference is the new term $d_2 e(t)\dot{x}$, which is responsible for coupling of energy depot on the particle motion and *vice versa*.

Majority of works on the subject of molecular motor relate to the overdamped case, *i.e.* the inertia term in the Langevin equation is usually skipped. This is a perfectly legitimate practice as a single Langevin equation in most of those works models behavior of a whole Brownian motor moving in a dense, viscous medium. However, inertial effects can be crucial for understanding processivity of non-biological nano-machines, as *e.g.* atomic motors moving in optical lattices [21]. There are also approaches which establish a connection between ABM dynamics and stochastic dynamics of a group of coupled molecular motors [28]. In contrast to models of overdamped dynamics, they incorporate more than just one equation of motion [29,27,28] while preserving also the inertia term. It should be stressed that including inertia $m\ddot{x}$ term in the Langevin equation implicates possible occurrence of chaotic behavior which has been documented in former studies on "inertia ratchet" models [30, 22]. The latter exhibit interesting performance characteristics, like negative mobility and current reversal.

In the case of motor proteins it seems also to be a wise choice to first model compartments of the protein with distinct Langevin equations and then, analyze the convergence of such a description to a single equation governing the motion of the center-of-mass. As a result, the center-of-mass dynamics can be associated with the single equation of motion considered in other models. The friction coefficient estimated in the center-of-mass implies a low ratio of the inertial and the viscous forces. In consequence, a low Reynolds number[9] is then the reason for skipping an inertia term.

The models discussed in this work have included inertia in the original equations of motion. Accordingly, for the purpose of achieving directed motion, values of initial conditions and other parameters controlling the motion have to be carefully adjusted. In the following section, an integral presentation of the models will be focused on defining range of parameters for which the motor works.

4.2. Ratchet model and motor efficiency

The relative motion of two heads (each of mass m) of the motor is given by [31, 32]

$$m\ddot{x} = -m\gamma_0\dot{x} - U'(x_c + x/2) + U'(x_c - x/2) + TS'(x) + mde(t)\dot{x} + m\sqrt{2D_v}\xi\,, \tag{13}$$

[9] The Reynolds number is equal to $R = \frac{\varrho L\dot{x}}{\zeta}$, where ϱ is the density of the medium, L is a characteristic length of the moving object, $\dot{x}$ is the speed of the movement relative to the medium and ζ stands for the viscosity.

where $U(x)$ is a ratchet-type periodic potential, friction frequency γ_0 is acting on the relative velocity v of the heads x, x_c stands for the position of kinesin's center-of-mass, $\xi(t)$ is a white Gaussian noise of intensity $m\sqrt{2D_v}$ with $D_v = \gamma_0 k_B T/m$ and $TS'(x)$ incorporates entropic force exerted by an extended elastomer that links motor heads, where $TS(x) = s_0 + ax^2 - bx^4$. The mechanical energy of motion is powered by the energy flow

$$\frac{de(t)}{dt} = q - ce(t) - mdv^2 e(t)\,, \tag{14}$$

with $v \equiv \dot{x}(t)$, q standing for energy accumulated in the depot container, c representing dissipation rate and d denoting coupling between the motor and the depot. An analogous equation for the motion of the center-of-mass reads [31]

$$v_c \equiv \dot{x}_c = \frac{1}{\Gamma}\left(F_0 - U'\left[x_c + \frac{x}{2}\right] - U'\left[x_c - \frac{x}{2}\right]\right) + \sqrt{2D_{x_c}}\xi_0\,, \tag{15}$$

where the total motor mass $M \gg 2m$ with $\Gamma\dot{x}_c$ denoting a viscous drag opposing the motion (here $\Gamma = 2M\Gamma_c$). In the above equation, F_0 stands for an additional force (load) disfavoring the movement of the motor and Γ_c denotes the friction coefficient in the center-of-mass [31]. For the ratchet potential $U(x)$ we use the standard model [33]

$$U(x) = h[0.499 - 0.453(\sin(2\pi(x+0.1903)) + \tfrac{1}{4}(\sin(2\pi(x+0.1903)))]\,, \tag{16}$$

where h is the height of the barriers. In this simple approach, efficiency of the motor can be estimated [34, 35] as a fraction of power exerted by the motor working against external force F_0 divided by the quanta of chemical energy q provided by the hydrolysis of ATP

$$\eta_C \equiv \frac{|F_0\langle v_c\rangle|}{q}\,. \tag{17}$$

The problem is, however, that in the absence of external force the efficiency is by definition zero. The way out is to follow the recipe presented by Derenyi *et al.* [36]. Those authors introduce the concept of *generalized efficiency*, defined as a ratio of minimal energy needed for the task to be accomplished (E_{in}) and the actual energy used to perform this task (E_{in})

$$\eta_{gen} \equiv \frac{E_{min}}{E_{in}}\,. \tag{18}$$

For molecular motors the minimal energy is used when the motor (interpreted as one body) is moving uniformly along the track at the average velocity $\langle v_c\rangle$. In this case the minimum power reads

$$P_{min} = \frac{dE_{min}}{dt} = F_0\langle v_c\rangle + \Gamma\langle v_c\rangle^2\,. \tag{19}$$

Consequently, the generalized efficiency for the presented model is defined as

$$\eta_{\mathrm{gen}} \equiv \frac{|F_0\langle v_{\mathrm{c}}\rangle| + \Gamma\langle v_{\mathrm{c}}\rangle^2}{q}\,, \tag{20}$$

where $\langle v_{\mathrm{c}}\rangle$ is an average velocity of the motor in the center-of-mass.

Yet another approach towards definition of the efficiency of molecular motors has been proposed in the papers by Wang *et al.* and Oster [35, 34]. Authors introduce so-called Stokes efficiency, viewed as a cost-effective measure of utilization by the motor of the chemical Gibbs free energy in generating a unidirectional motion and transporting a load through a viscous medium

$$\eta_{\mathrm{S}} \equiv \frac{\Gamma\langle v_{\mathrm{c}}\rangle^2}{A\langle r\rangle + F_0\langle v_{\mathrm{c}}\rangle}\,. \tag{21}$$

Here, A represents chemical free energy consumed in one motor cycle and $\langle r\rangle$ stands for the rate of the chemical reaction cycle. In terms of presented model the Stokes efficiency can be estimated by substituting $A\langle r\rangle = q$ in Eq. (21). To further inspect percentage of the free energy used by moving motor heads, we have also analyzed

$$\eta_{\mathrm{S}}^{\mathrm{heads}} \equiv \frac{m\gamma\langle|v|\rangle^2}{q + F_0\langle v_{\mathrm{c}}\rangle}\,, \tag{22}$$

where $\langle|v|\rangle$ stands for average absolute relative velocity of the motor heads. Figure 7 displays results of this analysis for a set of parameters guaranteeing the progressive motor's motion. The classical efficiency η_{C} gradually increases from a zero value to a maximum registered at $F_0 = 0.18$ followed by a subsequent drop to zero at a stall force $F_0 = 0.2$. Similar dependence of the efficiency with a maximum observed at moderate loads has been described in the experimental work of Nishiyama *et al.* [37].

In contrast, within the same range of load forces the Stokes efficiency η_{S} remains very low whereas the generalized definition Eq. (20) results in non-monotonous efficiency-load dependence. Altogether, this analysis shows importance of a proper definition of efficiency to be used when exploring energetics of molecular motors and making use of available experimental data. In particular, for motors with internal degrees of freedom, other channels for storage and dissipation of energy can be envisioned [38]. In such situations, the generalized definition of efficiency has to be tailored to take into account the average input power as the change in both, the potential and chemical energy of the motor cycle.

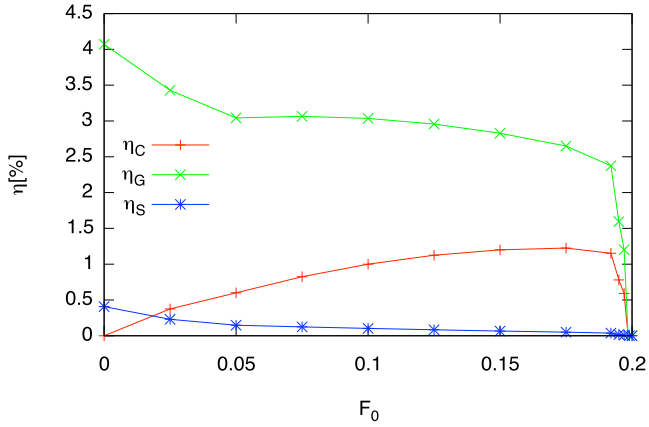

Fig. 7. Thermodynamical efficiency η_{C}, generalized efficiency η_{gen} and Stokes efficiency η_{S} as a function of the load force F_0, given in dimensionless units, for $\Gamma \approx 0.102$.

5. Conclusions

In general, molecular motors operate in groups performing dedicated tasks via synchronized action. In intracellular transport there is about several motors [3] which coordinate motion along microtubules. Many experiments and models have attempted to unravel basic features of load sharing and bi-directionality of the transport performed by higher assemblies of motors. Understanding collective behavior of molecular motors and nature of the protein friction associated with a directed motor motion are nowadays the most intriguing and important issues in this field.

Special thanks are directed to Martin Bier, East Carolina University, Greenville, for many inspiring and critical discussions on molecular motorics. The project has been supported by the European Science Foundation within the program EPSD (Exploring Physics of Small Devices). Authors (B.L. and E.G.-N.) additionally acknowledge funds from the Foundation for Polish Science (International Ph.D. Projects Program co-financed by the European Regional Development Fund covering, under the agreement No. MPD/2009/6; the Jagiellonian University International Ph.D. Studies in Physics of Complex Systems).

REFERENCES

[1] M.G.L. van den Heuvel, C. Dekker, *Science* **317**, 333 (2007).

[2] T. Kudernac *et al.*, *Nature* **479**, 208 (2011).

[3] J. Howard, *Mechanics of Motor Proteins and the Cytoskeleton*, Sinauer Associates Incorporated, new edition, 2001.

[4] T. Mitchison, M. Kirschner, *Nature* **312**, 237 (1984).

[5] V. Hariharan, W.O. Hancock, *Cell. Mol. Bioeng.* **2**, 177 (2009).

[6] P. Scherer, S. Fischer, *Theoretical Molecular Biophysics*, Springer Verlag, Berlin 2010.

[7] M.L. Kutys, J. Fricks, W.O. Hancock, *PLoS Comput. Biol.* **6**, 1 (2010).

[8] H. Berendsen, D. van der Spoel, R. van Drunen, *Comput. Phys. Commun.* **91**, 43 (1995).

[9] A. Yildiz, M. Tomishige, R. Vale, P. Selvin, *Science* **303**, 676 (2004).

[10] S. Liepelt, R. Lipowsky, *Phys. Rev. Lett.* **98**, 258102 (2007).

[11] N.R. Guydosh, S.M. Block, *Nature* **461**, 125 (2009).

[12] N.J. Carter, R.A. Cross, *Nature* **435**, 308 (2005).

[13] M. Bier, F.J. Cao, *Biosystems* **103**, 355 (2011).

[14] M. Fisher, A.B. Kolomeisky, *Proc. Natl. Acad. Sci. USA* **98**, 7748 (2001).

[15] B.E. Clancy *et al.*, *Nature Struct. Mol. Biol.* **18**, 1020 (2011).

[16] D.T. Gillespie, *J. Comput. Phys.* **22**, 403 (1976).

[17] D.T. Gillespie, *J. Phys. Chem.* **81**, 2340 (1977).

[18] R. Ellis, *Trends Biochem. Sci.* **26**, 597 (2001).

[19] M. Magnasco, *Phys. Rev. Lett.* **71**, 1477 (1993).

[20] R.D. Astumian, *Biophys. J.* **98**, 2401 (2010).

[21] P. Hänggi, F. Marchesoni, *Rev. Mod. Phys.* **81**, 387 (2009).

[22] L. Machura, M. Kostur, J. Łuczka, *Biosystems* **94**, 253 (2008).

[23] P. Reimann, *Phys. Rep.* **361**, 57 (2002).

[24] F. Schweitzer, W. Ebeling, B. Tilch, *Phys. Rev. Lett.* **80**, 5044 (1998).

[25] A. Fiasconaro, E. Gudowska-Nowak, W. Ebeling, *J. Stat. Mech.: Theory Exp.* **P01029**, (2009).

[26] W. Ebeling, E. Gudowska-Nowak, A. Fiasconaro, *Acta Phys. Pol. B* **39**, 1251 (2008).

[27] B. Lindner, *New J. Phys.* **12**, 063026 (2010).

[28] C. Touya, T. Schwalger, B. Lindner, *Phys. Rev.* **E83**, 051913 (2011).

[29] I. Derenyi, T. Vicsek, *Proc. Natl. Acad. Sci. USA* **93**, 6775 (1996).

[30] M. Kostur, P. Hänggi, P. Talkner, J. Mateos, *Phys. Rev.* **E72**, 036210 (2005).

[31] M.A. Żabicki, W. Ebeling, E. Gudowska-Nowak, *Chem. Phys.* **375**, 472 (2010).

[32] M.A. Żabicki, E. Gudowska-Nowak, W. Ebeling, *Acta Phys. Pol. B* **41**, 1181 (2010).

[33] J.L. Mateos, *Acta Phys. Pol. B* **32**, 307 (2001).

[34] H. Wang, G. Oster, *Europhys. Lett.* **57**, 134 (2002).

[35] J. Wang, *ACS Nano.* **3**, 4 (2009).

[36] I. Derenyi, M. Bier, R.D. Astumian, *Phys. Rev. Lett.* **83**, 903 (1999).

[37] M. Nishiyama, H. Higuchi, T. Yanagida, *Nat. Cell. Biol.* **4**, 11782 (2002).

[38] H. Linke, M.T. Downton, M.J. Zuckermann, *Chaos: Interdisciplin. J. Nonlinear Sci.* **15**, 026111 (2005).